

# Entangled Dilaton Dyons

---

**Nilay Kundu<sup>1</sup>, Prithvi Narayan<sup>1</sup>, Nilanjan Sircar<sup>1</sup> and Sandip P. Trivedi<sup>1</sup>**

<sup>1</sup>*Tata Institute for Fundamental Research  
Mumbai 400005, India*

Email: nilay.tifr@gmail.com, prithvi.narayan@gmail.com,  
nilanjan.tifr@gmail.com, trivedi.sp@gmail.com

**ABSTRACT:** Einstein-Maxwell theory coupled to a dilaton is known to give rise to extremal solutions with hyperscaling violation. We study the behaviour of these solutions in the presence of a small magnetic field. We find that in a region of parameter space the magnetic field is relevant in the infra-red and completely changes the behaviour of the solution which now flows to an  $AdS_2 \times R^2$  attractor. As a result there is an extensive ground state entropy and the entanglement entropy of a sufficiently big region on the boundary grows like the volume. In particular, this happens for values of parameters at which the purely electric theory has an entanglement entropy growing with the area,  $A$ , like  $A \log(A)$  which is believed to be a characteristic feature of a Fermi surface. Some other thermodynamic properties are also analysed and a more detailed characterisation of the entanglement entropy is also carried out in the presence of a magnetic field. Other regions of parameter space not described by the  $AdS_2 \times R^2$  end point are also discussed.

---

## Contents

<b>1. Introduction</b>	<b>1</b>
1.1 Key Results	3
<b>2. The Dilaton Gravity System</b>	<b>5</b>
2.1 Solutions With Only Electric Charge	6
<b>3. The Effect of the Magnetic field</b>	<b>9</b>
3.1 Case I. $-\delta < \alpha < 0$	10
3.2 Case II. $ \alpha  > \delta$	10
3.3 Case III. $0 < \alpha < \delta$	12
3.4 Additional Comments	13
<b>4. More on Thermodynamics</b>	<b>13</b>
4.1 More on Case II.	16
<b>5. Entanglement Entropy</b>	<b>18</b>
5.1 Entanglement Entropy in Hyperscaling Violating Metrics	18
5.2 Entanglement with a Small Magnetic Field	22
<b>6. Concluding Comments</b>	<b>23</b>
<b>A. Appendix : Numerical Interpolation.</b>	<b>26</b>
A.1 The perturbations	26
A.2 Scaling symmetries	27
A.3 Numerics : $AdS_2 \times R^2$ to the Electric Scaling Solution	27
A.4 Numerics : $AdS_2 \times R^2 \rightarrow$ Electric Scaling $\rightarrow AdS_4$ .	28

---

## 1. Introduction

The AdS/CFT correspondence suggests that interesting connections could arise between gravitation and condensed matter physics. An important class of systems in condensed matter physics which one could try and study using this correspondence consists of fermions at finite density with strong correlations. Landau Fermi liquid theory is one paradigm that often describes such systems, but it can fail. The

resulting Non-Fermi liquid behaviour is poorly understood and believed to be of considerable interest, e.g., in the study of High  $T_c$  superconductors in  $2 + 1$  dimensions.

On the gravity side, the Einstein Maxwell Dilaton (EMD) system consisting of gravity and a Maxwell gauge field coupled to a neutral scalar (the Dilaton) is of considerable interest from the point of view of studying this problem. Fermions in the boundary theory carry a conserved charge - fermion number- so it is natural to include a gauge field in the bulk. The presence of a neutral scalar allows for promising new phases to arise where the entropy vanishes at non-zero chemical potential and zero temperature, as was discussed in [1], [2], [3]. These phases correspond to compressible states of matter with unbroken fermion number symmetry <sup>1</sup>. It was found that the thermodynamics and transport properties of these systems, while showing the existence of gapless excitations, do not fit those of a Landau Fermi liquid. For example, the specific heat is typically not linear in the temperature ( $T$ ), at small temperatures, and the electric resistivity also does not have the required  $T^2$  dependence <sup>2</sup>.

An exciting recent development has shown that for an appropriate range parameters such an EMD system could give rise to an entanglement entropy which reproduces the behaviour expected of a system with a Fermi surface. If we take a sufficiently big region in space in a system with a Fermi surface it is believed that the entanglement entropy goes like

$$S_{entangled} \sim A \log(A) \tag{1.1}$$

where  $A$  is the area of the boundary of this region <sup>3</sup>. The log enhancement is believed to be the tell-tale signature of a Fermi surface. Exactly such a behaviour was shown to arise for appropriate choices of parameters in the EMD system in [10], see also [11]. In addition, it was argued that the specific heat, at small temperatures, could be understood on the basis of gapless excitations which dispersed with a non-trivial dynamical exponent.

Taken together, these developments suggest that for an appropriate range of parameters the EMD system could perhaps describe phases where a Fermi surface does form but where the resulting description is not of Landau Fermi liquid type. While this is a promising possibility it is far from being definitely established. In fact, as has been known for some time now, at large  $N$  (classical gravity) the system does not exhibit some of the standard characteristics expected of a system with a

---

<sup>1</sup>The significance of the compressible nature of the state was emphasised to us by S. Sachdev, see [4].

<sup>2</sup>These results refer to the case when the boundary theory is  $2 + 1$  dimensional with a  $3 + 1$  dimensional bulk dual.

<sup>3</sup>Strictly speaking this behaviour has only been proven for free or weakly coupled fermions [5],[6] but it is expected to be more generally true due to the locus of gapless excitations which arises in the presence of a Fermi surface. Additional evidence has also been obtained in [7], [8], [9].

Fermi surface. For example there are no oscillations in the magnetisation and other properties as the magnetic field is varied (the de Haas-van Alphen effect) , nor are there any  $2k_F$  Friedel oscillation <sup>4</sup>. More recently the non-zero momentum current-current two point function has been calculated and found to have suppressed weight at small frequency [14].

In this paper we will continue to study this class of systems from the gravity side by turning on an additional magnetic field and determining the resulting response. In our work the magnetic field will be kept small compared to charge density in the boundary theory. We will be more specific about what this means in terms of the energy scales of the boundary theory shortly. For now let us note that without a magnetic field the purely electric theory has a scaling-type solution (more correctly a hyperscaling violating solution). The magnetic field is kept small so that its effects are a small perturbation compared to the electric field in the ultraviolet (UV) of this scaling solution.

## 1.1 Key Results

For a conventional Fermi liquid (see for example chapter 14 of [15]), the introduction of a small magnetic field does not do anything drastic. In particular the Fermi surface is not destroyed by it. The thermodynamic entropy receives only small corrections and the specific heat at small temperatures continues to be linear in  $T$ . The presence of the Fermi surface should also mean that the entanglement entropy continues to have the logarithmic enhancement eq.(1.1).

In contrast, we find that in the dilaton system even a small magnetic field can have a dramatic effect since it can become relevant in the Infra-red (IR). The resulting thermodynamic and entanglement entropy can then change drastically. In particular this happens for the whole range of parameters where the entanglement entropy is of the form eq.(1.1).

More specifically, the EMD system we analyse is characterised by two parameters  $(\alpha, \delta)$  which are defined in <sup>5</sup> eq.(2.2), eq.(2.3).

When  $|\alpha| > |\delta|$  we show that the magnetic field is relevant in the IR and the geometry in the deep infra-red (small values of the radial coordinate  $r$  we use ) flows to an  $AdS_2 \times R^2$  attractor. As a result the system acquires a non-zero extensive entropy even at zero temperature. The entanglement entropy also changes and grows like the volume of the region of interest <sup>6</sup> (for large enough volume). In particular,

---

<sup>4</sup>At one loop de Haas- van Alphen type oscillations are seen, [12]. For some recent discussion of Friedel oscillations in  $(1+1)$  dim. see [13].

<sup>5</sup>The relation of  $(\alpha, \delta)$  to the parameters  $(\theta, z)$  now more conventionally used in the literature is given in eq.(2.29). In particular  $\alpha = -3\delta$  corresponds to  $\theta = d - 1 = 1$ .

<sup>6</sup>A potential confusion with our terminology arises because we are in two dimensions. Thus the volume of the region of interest is actually its area and the area of the boundary of this region is the perimeter.

this happens for the values  $\alpha = -3\delta$  where the purely electric theory gives rise to an entanglement of the form eq.(1.1).

As we discussed, the  $A \log(A)$  behaviour of the entanglement entropy is believed to be a signature for the presence of a Fermi surface. Our result that a small magnetic field alters the entanglement entropy drastically suggests that the putative Fermi surface is destroyed by even a very weak magnetic field in this state.

We also analyse the thermodynamics and some transport properties of the resulting state. The system continues to be compressible in the presence of a magnetic field and its specific heat is linear at small temperatures. Both these facts indicate the presence of gapless excitations. In general the system has a magnetisation which is linear in the magnetic field and which is expected to be diamagnetic. The  $AdS_2 \times R^2$  attractor leads to the magnetisation having a temperature dependence, at small  $T$ , which can become important even for small magnetic fields, eq.(4.17).

The summary is that for parameters where the electric theory has an entanglement of the form eq.(1.1), suggesting that it is a non-Landau Fermi liquid, the magnetic field is a relevant perturbation in the IR. As a result even a small magnetic field has a dramatic effect on the state of the system. The state continues to be compressible, with a linear specific heat, but the thermodynamic entropy at zero temperature is now extensive and the entanglement entropy scales like the volume of the region of interest. These results suggests that the Fermi surface if present in the electric theory is fragile and destroyed by even a small magnetic field. More generally from the fact that the magnetic field is a relevant perturbation in the IR we learn that the compressible state described by the purely electric solution “anti-screens” the effects of the magnetic field making them grow at larger distances. Similar results for the existence of an  $AdS_2 \times R^2$  attractor and associated changes in thermodynamic and entanglement entropy etc are true in the whole region where  $|\alpha| > |\delta|$ .

In other regions of parameter space where  $|\alpha| < |\delta|$  the magnetic perturbation is either not relevant in the IR and thus essentially leaves the low-energy and large distance behaviour of the system unchanged. Or it is relevant but we have not been able to completely establish the resulting geometry to which the system flows in the deep IR.

The paper is planned as follows. We start with a brief description of the dilatonic system and the hyperscaling violating metrics in §2. The effects of a magnetic field are discussed in §3. The resulting thermodynamics is discussed in §4 and the entanglement entropy in §5. We end with a discussion of results and some concluding comments in §6. Appendix A contains important details about the numerical analysis.

Before ending the introduction let us also comment on some related literature. For a discussion of probe fermions in the extremal RN geometry and the resulting non-Fermi liquid behaviour see, [16],[17], [18],[19],[20],[21]. The EMD system has been studied in [1],[2],[3],[22],[23],[24],[25],[26],[27],[28]. The subject of entanglement

entropy has received considerable attention in the literature lately, for a partial list of references see [29],[30],[31], [32],[33], for early work; and for a discussion within the context of the AdS/CFT correspondence see [34],[35] .

Two papers in particular have overlap with the work reported here. While their motivations were different the analysis carried out in these papers is similar to ours. The EMD system with the inclusion of possible higher order corrections was analysed in [36] and it was found that sometimes these corrections could change the behaviour of the geometry resulting in an  $AdS_2 \times R^2$  region in the deep IR. This analysis was generalised to the case with hyperscaling violation in the more recent paper [37] which appeared while our work was being completed.

## 2. The Dilaton Gravity System

We work in  $3 + 1$  dimensions in the gravity theory with an action

$$S = \int d^4x \sqrt{-g} [R - 2(\nabla\phi)^2 - f(\phi)F_{\mu\nu}F^{\mu\nu} - V(\phi)]. \quad (2.1)$$

Much of our emphasis will be on understanding the near horizon region of the black brane solutions which arise in this system. This region is more universal, often having the properties of an attractor, and also determines the IR behaviour of the system. In this region, in the solutions of interest, the dilaton will become large,  $\phi \rightarrow \pm\infty$ . The potential and gauge coupling function take the approximate forms

$$f(\phi) = e^{2\alpha\phi} \quad (2.2)$$

$$V = -|V_0|e^{2\delta\phi} \quad (2.3)$$

along this direction of field space. The two parameters,  $\alpha, \delta$ , govern the behaviour of the system. For example the thermodynamic and transport properties and also the entanglement properties crucially depend on these parameters. The action in eq. (2.1) has a symmetry under which the sign of  $\phi, \alpha, \delta$  are reversed. Without loss of generality we will therefore choose  $\delta > 0$  in the discussion which follows.

Our analysis will build on the earlier investigations in [3] and [26], and our conventions will be those in [26]. We will work in coordinates where the metric is,

$$ds^2 = -a(r)^2 dt^2 + \frac{dr^2}{a(r)^2} + b(r)^2(dx^2 + dy^2) \quad (2.4)$$

The horizon of the extremal black brane will be taken to lie at  $r = 0$ .

The gauge field equation of motion gives,

$$F = \frac{Q_e}{f(\phi)b^2} dt \wedge dr + Q_m dx \wedge dy. \quad (2.5)$$

The remaining equations of motion can be conveniently expressed in terms of an effective potential [38]

$$V_{\text{eff}} = \frac{1}{b^2} (e^{-2\alpha\phi} Q_e^2 + e^{2\alpha\phi} Q_m^2) - \frac{b^2 |V_0|}{2} e^{2\delta\phi}, \quad (2.6)$$

and are given by,

$$(a^2 b^2)'' = 2|V_0| e^{2\delta\phi} b^2 \quad (2.7)$$

$$\frac{b''}{b} = -\phi'^2 \quad (2.8)$$

$$(a^2 b^2 \phi')' = \frac{1}{2} \partial_\phi V_{\text{eff}} \quad (2.9)$$

$$a^2 b'^2 + \frac{1}{2} a'^2 b'^2 = a^2 b^2 \phi'^2 - V_{\text{eff}}. \quad (2.10)$$

## 2.1 Solutions With Only Electric Charge

Next let us briefly review the solutions with  $Q_m$  set to zero which carry only electric charge. The solution in the near-horizon region take the form,

$$a = C_a r^\gamma \quad b = r^\beta \quad \phi = k \log r \quad (2.11)$$

where the coefficients  $C_a, \gamma, \beta, k$  and the electric charge  $Q_e$  are given by

$$\begin{aligned} \beta &= \frac{(\alpha + \delta)^2}{4 + (\alpha + \delta)^2} & \gamma &= 1 - \frac{2\delta(\alpha + \delta)}{4 + (\alpha + \delta)^2} & k &= -\frac{2(\alpha + \delta)}{4 + (\alpha + \delta)^2} \\ C_a^2 &= |V_0| \frac{(4 + (\alpha + \delta)^2)^2}{2(2 + \alpha(\alpha + \delta))(4 + (3\alpha - \delta)(\alpha + \delta))} & Q_e^2 &= |V_0| \frac{2 - \delta(\alpha + \delta)}{2(2 + \alpha(\alpha + \delta))}. \end{aligned} \quad (2.12)$$

It might seem strange at first that the electric charge  $Q_e$  is fixed, this happens because in the near-horizon metric we work with the the time (and spatial coordinates) which have been rescaled compared to their values in the UV.

The following three conditions must be satisfied for this solution to be valid :  $Q_e^2 > 0, C_a^2 > 0, \gamma > 0$ . These give the constraints,

$$2 - \delta(\alpha + \delta) > 0 \quad (2.14)$$

$$2 + \alpha(\alpha + \delta) > 0 \quad (2.15)$$

$$4 + (3\alpha - \delta)(\alpha + \delta) > 0 \quad (2.16)$$

$$4 + (\alpha - 3\delta)(\alpha + \delta) > 0. \quad (2.17)$$

The last of these conditions follow from the requirement that

$$2\gamma - 1 > 0 \quad (2.18)$$

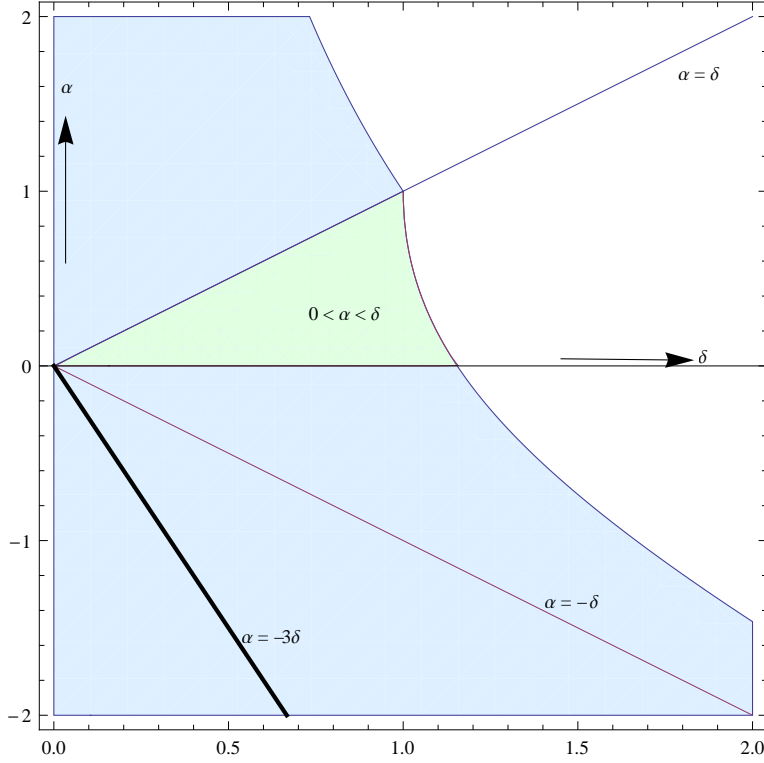


**Figure 1:** Figure showing the region of  $(\delta, \alpha)$  space allowed by various positivity and thermodynamics constraints for electric scaling solution

so that the specific heat is positive. Figure (1) shows the the region in the  $(\delta, \alpha)$  plane, with  $\delta > 0$ , allowed by the above constraints.

To summarise our discussion, the metric in the purely electric solution takes the form

$$ds^2 = -C_a^2 r^{2\gamma} dt^2 + \frac{dr^2}{C_a^2 r^{2\gamma}} + r^{2\beta} (dx^2 + dy^2). \quad (2.19)$$

And the dilaton is given in eq.(2.11,2.12) While this solution is not scale invariant it does admit a conformal killing vector. This follows from noting that under the transformation

$$r = \lambda \tilde{r} \quad (2.20)$$

$$t = \lambda^{1-2\gamma} \tilde{t} \quad (2.21)$$

$$\{x, y\} = \lambda^{1-\gamma-\beta} \{\tilde{x}, \tilde{y}\} \quad (2.22)$$

the metric eq.(2.19) remains invariant upto a overall scaling,

$$ds^2 = \lambda^{2-2\gamma} \left\{ -C_a^2 \tilde{r}^{2\gamma} d\tilde{t}^2 + \frac{d\tilde{r}^2}{C_a^2 \tilde{r}^{2\gamma}} + \tilde{r}^{2\beta} (d\tilde{x}^2 + d\tilde{y}^2) \right\}. \quad (2.23)$$



The dilaton also changes under this rescaling by an additive constant,

$$\phi = k \ln(\tilde{r}) + k \ln(\lambda) \quad (2.24)$$

The two exponents  $\gamma, \beta$  which appear in the metric are related to the dynamic exponent with which gapless excitations disperse and hyperscaling violations, as was explained in [11].

Under the coordinate change,

$$r = \tilde{r}^{-\frac{1}{\beta}} \quad (2.25)$$

$$t = \frac{1}{\beta C_a^2} \tilde{t} \quad (2.26)$$

$$(x, y) = \frac{1}{\beta C_a} (\tilde{x}, \tilde{y}), \quad (2.27)$$

the metric eq.(2.19) becomes

$$ds^2 = \frac{1}{\beta^2 C_a^2} \frac{1}{\tilde{r}^2} \left\{ -\frac{d\tilde{t}^2}{\tilde{r}^{\frac{4(z-1)}{2-\theta}}} + \tilde{r}^{\frac{2\theta}{2-\theta}} d\tilde{r}^2 + d\tilde{x}^2 + d\tilde{y}^2 \right\}. \quad (2.28)$$

Where,

$$z = \frac{2\gamma - 1}{\beta + \gamma - 1} \quad \theta = \frac{2(\gamma - 1)}{\beta + \gamma - 1}. \quad (2.29)$$

This is the form of the metric discussed in [11] (upto the overall  $\frac{1}{\beta^2 C_a^2}$  factor which was set to unity by a choice of scale). The exponent  $z$  is the dynamic exponent, as we can see from the scaling weights of the  $t$  and  $x, y$  directions in eq.(2.21), eq.(2.22). The exponent  $\theta$  is the hyperscaling violation exponent, we will also explain this further in §4.

Let us end this section with some more comments. In eq.(2.5) the two-form  $F$  is dimensionless, so that  $Q_e, Q_m$  have dimensions of  $[Mass]^2$ . The chemical potential  $\mu$  is related to  $Q_e$  by

$$Q_e \sim \mu^2 \quad (2.30)$$

and has dimensions of mass.

The near-horizon geometry of the type being discussed here can be obtained by starting from an asymptotically AdS space in the UV for a suitable choice of the potential  $V(\phi)$ . This was shown, e.g., in [26], for additional discussion see Appendix A. It is simplest to consider situations where the asymptotic AdS space has only one scale,  $\mu$ , which characterises both the chemical potential of the boundary theory and any breaking of conformal invariance due to a non-normalisable mode for the dilaton being turned on. In our subsequent discussion we will have such a situation in mind and the scale  $\mu$  will often enter the discussion of the thermodynamics and entanglement.

Also note that the parameter  $N^2$  which will enter for example in the entropy eq.(4.7) is given in terms of the potential eq.(2.3) by

$$N^2 \sim \frac{1}{G_N |V_0|}. \quad (2.31)$$

Again to keep the discussion simple we will take the cosmological constant for the asymptotic  $AdS$  to be of order  $V_0$  so that  $N^2$  is also number of the degrees of freedom in the UV<sup>7</sup>.

The solutions we have considered can have curvature singularities as  $r \rightarrow 0$ , when such singularities are absent tidal forces can still diverge near the horizon, e.g., see <sup>8</sup>, [40]. These divergences can be cut-off by heating the system up to a small temperature as discussed in [2], [26]. Also, as we will see shortly, adding a small magnetic field can alter the behaviour of the geometry in the deep IR again removing the singular region.

### 3. The Effect of the Magnetic field

Now that we have understood the solutions obtained with only electric charge we are ready to study the effects of adding a small magnetic field.

The presence of the magnetic field gives rise to an additional term in the effective potential eq.(2.6). The magnetic field is a small perturbation if this term is small compared to the electric charge term, giving rise to the condition

$$\left(\frac{Q_m}{Q_e}\right)^2 \ll e^{-4\alpha\phi}. \quad (3.1)$$

From eq.(2.11) and eq.(2.12) we see that

$$e^{-4\alpha\phi} = r^{-4\alpha k} \quad (3.2)$$

so eq.(3.1) in fact gives rise to a condition on the radial coordinate

$$\left(\frac{Q_m}{Q_e}\right)^2 \ll r^{-4\alpha k}. \quad (3.3)$$

By a small magnetic field we mean more precisely choosing a suitable value of  $Q_m$  and starting at a value of the radial coordinate  $r$  where eq.(3.3) is met. We will

---

<sup>7</sup>The examples studied in [26] are of this type. There the full potential was taken to be  $V(\phi) = -2|V_0| \cosh(2\delta\phi)$  (see eq.(F.1 of [26])). As a result in the asymptotic region  $r \rightarrow \infty$  the potential goes to its maximum value,  $V \rightarrow V_\infty = -2|V_0| \sim -|V_0|$ .

<sup>8</sup>Sometimes the geometries can be regular with no singularities or diverging tidal forces, [39].

be then interested in asking if this magnetic perturbation continues to be small in the IR, i.e., even smaller values of  $r$ , or if its effects grow <sup>9</sup>.

The requirement that the magnetic field is small can be stated more physically as follows. Consider a purely electric solution which asymptotes to  $AdS$  space in the far UV and let  $\mu$  be the only scale characterising the boundary theory which is dual to this electric theory as discussed in the previous section. Then the magnetic field is small if it satisfies the condition

$$|Q_m| \ll \mu^2, \quad (3.4)$$

so that its effects can be neglected in the UV and continue to be small all the way to the electric scaling region.

Our discussion breaks up into different cases depending on the values of the parameters  $\alpha, \delta$ . We will choose  $\delta \geq 0$  in the discussion below without any loss of generality. Let us also note that although we do not always mention them for an electric solution to exist the additional conditions eq.(2.14)-eq.(2.17) must also be met.

We now turn to the various cases.

### 3.1 Case I. $-\delta < \alpha < 0$

In this case the magnetic perturbation is irrelevant in the infrared. From eq.(2.12) we see that  $\alpha k > 0$  so that

$$e^{-4\alpha\phi} = r^{-4\alpha k} \rightarrow \infty \quad (3.5)$$

as  $r \rightarrow 0$ . Thus choosing a value of  $Q_m, r$ , where eq.(3.1) is met and going to smaller values of  $r$ , eq.(3.1) will continue to hold and therefore the effects of the magnetic field will continue to be small <sup>10</sup>. In this range of parameters then the low temperature behaviour of the system and its low frequency response will be unchanged from the purely electric case. Also the entanglement entropy in the boundary theory of a region of sufficient large volume will be unchanged and be given as we shall see in §5 by eq.(5.16).

### 3.2 Case II. $|\alpha| > \delta$

In this case the magnetic perturbation is relevant in the infrared and in the deep infrared the solution approaches an attractor of the extremal RN type. The dilaton

---

<sup>9</sup>As is clear from eq.(3.3) and we will study this shortly in more detail, the magnetic field is relevant in the IR when  $\alpha k < 0$ . It is easy to see from eq.(2.12), eq.(2.13) that when this condition is met the coupling  $g^2 = e^{-2\alpha\phi}$  in the purely electric solution is weakly coupled in the IR since  $g^2 \rightarrow 0$  as  $r \rightarrow 0$ .

<sup>10</sup>On the other hand the magnetic field gets increasingly more important at large  $r$ , i.e., in the UV. However from numerical solutions one sees that for a suitable  $V(\phi)$ , when  $Q'_m \mu^2 \ll 1$  its effects continue to be small all the way upto the asymptotic AdS region.

is drawn to a fixed and finite value  $\phi_0$  and does not run-away and the near-horizon geometry is  $AdS_2 \times R^2$  with the metric components eq.(2.4), being

$$b = b_0 \quad (3.6)$$

$$a^2 = \frac{r^2}{R_2^2}, \quad (3.7)$$

where  $b_0, R_2^2$  are constants with  $R_2$  being the radius of  $AdS_2$ . Note that in this attractor region of the spacetime the effects of the electric and magnetic fields are comparable.

To establish this result we first show that eq.(2.7), eq.(2.8), eq.(2.9) and eq.(2.10) allow for such an attractor solution. Next, starting with this attractor solution we identify appropriate perturbations and establish numerically that the solution flows to the electric scaling solution in the UV.

It is easy to check that the equations of motion allow for a solution of the type described above. Eq.(2.9) and eq.(2.10) are met with  $\phi$  being constant and  $b$  being constant as long as the conditions  $V_{eff} = \partial_\phi V_{eff} = 0$  are met. This gives rise to the conditions

$$e^{-2\alpha\phi_0} Q_e^2 + e^{2\alpha\phi_0} Q_m^2 = \frac{b_0^4 |V_0|}{2} e^{2\delta\phi_0} \quad (3.8)$$

$$-e^{-2\alpha\phi_0} Q_e^2 + e^{2\alpha\phi_0} Q_m^2 = \left(\frac{\delta}{\alpha}\right) \frac{b_0^4 |V_0|}{2} e^{2\delta\phi_0} \quad (3.9)$$

which determine  $\phi_0, b_0$ . Eliminating  $b_0$  between the two equations gives

$$e^{4\alpha\phi_0} = \frac{Q_e^2}{Q_m^2} \frac{1 + \frac{\delta}{\alpha}}{1 - \frac{\delta}{\alpha}} \quad (3.10)$$

The LHS must be positive, this gives a constraint  $|\frac{\delta}{\alpha}| < 1$  which is indeed true for Case II. Substituting eq.(3.10) in eq.(3.8) next determines  $b_0$  in terms of  $\phi_0$  to be

$$b_0^4 = \frac{4Q_e^2 e^{-2\phi_0(\alpha+\delta)}}{|V_0| \left(1 - \frac{\delta}{\alpha}\right)}. \quad (3.11)$$

Of the remaining equations eq.(2.8) is trivially satisfied while eq.(2.7) determines  $R_2$  to be

$$R_2^2 = \frac{1}{|V_0|} \left(\frac{\alpha - \delta}{\alpha + \delta}\right)^{\frac{\delta}{2\alpha}} \left(\frac{Q_m^2}{Q_e^2}\right)^{\frac{\delta}{2\alpha}}. \quad (3.12)$$

We see that  $R_2 \rightarrow 0$  as  $Q_m \rightarrow 0$ , making the  $AdS_2$  highly curved, while for  $\alpha > 0$   $R_2 \rightarrow \infty$  as  $Q_m \rightarrow 0$ .

Appendix A contains some discussion of the two perturbations in this  $AdS_2 \times R^2$  solution which grow in the UV. Starting with an appropriate choice of these two perturbations we find that the solution flows to the electric scaling solution in the

UV. This can be seen in Fig. (4) and (5). For an appropriate choice of potential going out even further in the UV one finds that the solution becomes asymptotically  $AdS_4$ , as shown in Fig. (7) and (8).

The  $AdS_2 \times R^2$  near-horizon geometry changes the IR behaviour of the system completely. As discussed in the introduction there is now an extensive thermodynamic entropy and the entanglement entropy also scales like the volume, for large enough volume. For additional discussion of the thermodynamics see §4 .

### 3.3 Case III. $0 < \alpha < \delta$

In this case also we will see that the magnetic perturbation is relevant in the IR. Our analysis for what the end point is in the IR will not be complete, however.

We do identify a candidate “run-away” attractor as the IR end point of the system. In this attractor solution the magnetic field dominates and the effects of the electric field are negligible in comparison. As a result a solution taking the hyper-scaling violating form eq.(2.11), for an appropriate choice of exponents, exists. We will refer to this solution as the magnetic scaling solution below. Unfortunately, we have not been able to satisfactorily establish that starting with the electric solution of interest one does indeed end in this magnetic scaling solution in the IR. This requires additional numerical work.

To see that the magnetic perturbation is relevant in the IR note that  $\alpha k < 0$  in this region so that eventually, for small enough values of  $r$ , condition eq.(3.3) will no longer hold and the effects of the magnetic field will become significant.

To identify the candidate run-away attractor let us begin by noting that the effective potential eq.(2.6) and thus the equations of motion are invariant under the transformation,  $Q_m \leftrightarrow Q_e$  accompanied by  $\alpha \rightarrow -\alpha$  with the other parameters staying the same. Under this transformation the region discussed in Case I maps to the region  $0 < \alpha < \delta$ . The discussion for Case I above then shows that, with  $Q_m$  present, in this region of parameter space there is a consistent solution where the effects of the electric charge in the deep IR can be neglected. The solution takes the form, eq.(2.11) and eq.(2.12), eq.(2.13), with  $Q_e \rightarrow Q_m$  and  $\alpha \rightarrow -\alpha$ . This is the magnetic scaling solution referred to above. Actually, this solution exists only if  $(-\alpha, \delta)$  meet the conditions eq.(2.14)-eq.(2.17). From Fig.(1) it is easy to see that this is true if  $(\alpha, \delta)$  lies in Case III and meets the conditions eq.(2.14)-eq.(2.17) in the first place.

Assuming that we have identified the correct IR end point we see that the thermodynamic entropy at extremality continues to vanish once the magnetic perturbation is added. It is also easy to see that the entanglement entropy is of the form eq.(5.16).

A more complete analysis of the system in this region of  $(\alpha, \delta)$  parameter space is left for the future.

### 3.4 Additional Comments

We end this section with some comments. It is sometimes useful to think of the solutions we have been discussing as being embedded in a more complete one which asymptotes to AdS space in the UV. The dual field theory then lives on the boundary of AdS space and standard rules of AdS/CFT can be used to understand its behavior. We take this theory to have one scale,  $\mu$ , as discussed in §2. In addition the magnetic field is also turned on with  $Q_m/\mu^2 \ll 1$ . The full metric for this solution will be of the form eq.(2.4) and in the UV will become AdS space <sup>11</sup> :

$$ds^2 = -r^2 dt^2 + \frac{1}{r^2} dr^2 + r^2(dx^2 + dy^2) \quad (3.13)$$

Starting with this geometry for  $r \rightarrow \infty$  it will approach the electric scaling solution when  $r \lesssim \mu$ .

The magnetic field becomes a significant effect when its contribution to the effective potential eq.(2.6) is roughly comparable to the electric field. This gives a condition for the dilaton

$$e^{-4\alpha\phi} \sim \frac{Q_m^2}{Q_e^2} \quad (3.14)$$

Using eq.(2.12) this happens at a radial location  $r \sim r_*$  where

$$r_* \sim \mu \left( \frac{Q_m^2}{Q_e^2} \right)^{\frac{-1}{4\alpha k}} \quad (3.15)$$

Here we have introduced the parameter  $\mu$  which was set equal to unity in eq.(2.11), eq.(2.12), eq.(2.13). For Case II and III where the magnetic perturbation is relevant in the IR,  $\alpha k < 0$ , and the magnetic field continues to be important for all  $r < r_*$ . In Case II for  $r \ll r_*$  the solution becomes  $AdS_2 \times R^2$ . In Case III we have not identified the IR endpoint with certainty when  $r \ll r_*$ . For Case I the magnetic perturbation is irrelevant in the IR.

Second, Figure (2) shows a plot of various regions in the  $(\delta, \alpha)$  plane, with  $\delta > 0$ . Region C corresponds to Case I. Regions A, D and E correspond to Case II. And region B corresponds to Case III. The line  $\alpha = -3\delta$  which is of special interest is the thick black line separating regions E and D. These regions are also described in terms of the parameters  $\beta, \gamma$ , eq.(2.12), eq.(2.13) in Table (1). The corresponding values of the parameters  $(\theta, z)$  can be obtained from eq.(2.29).

## 4. More on Thermodynamics

In this section we will discuss the thermodynamic behaviour in the presence of the magnetic field in some more detail. For a conventional Landau Fermi liquid the presence of a small magnetic field does not drastically change the behaviour of the system

---

<sup>11</sup>We have set  $R_{AdS} = 1$ .

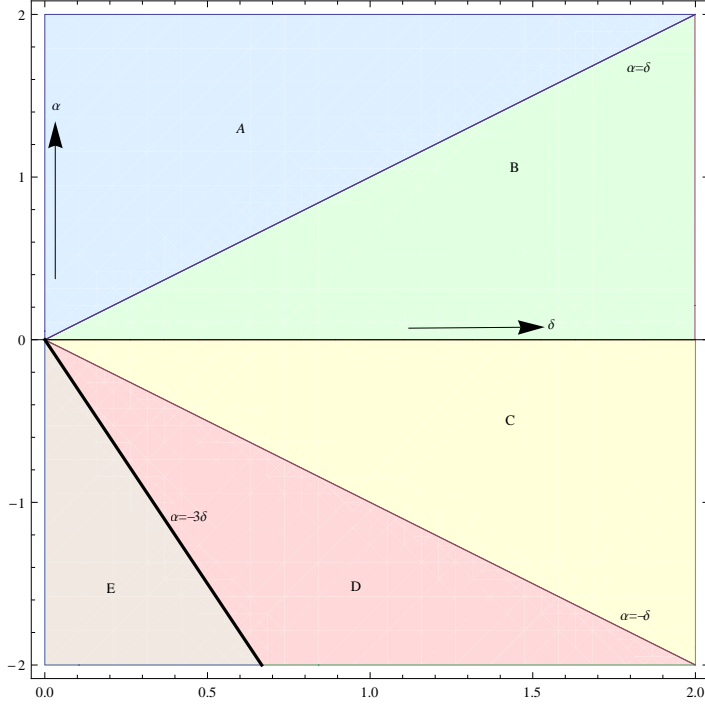


**Figure 2:** Figure showing various region in  $(\delta, \alpha)$  space. Details of these regions can be found in Table (1)

Region	$\delta, \alpha$	$\beta, \gamma$
A	$\alpha > \delta$	$1 + \beta > \gamma > 1 - \beta$
B	$0 < \alpha < \delta$	$\gamma < 1 - \beta$
C	$0 > \alpha > -\delta$	$\gamma < 1 - \beta$
D	$-3\delta < \alpha < -\delta$	$\gamma > 1 + \beta$
E	$\alpha < -3\delta$	$1 + \beta > \gamma > 1 - \beta$

**Table 1:** Various Regions in  $(\delta, \alpha)$  space

as was mentioned in the introduction. In particular, the Fermi surface is left intact by such a field. As a result the specific heat is still linear for small temperatures, with small magnetic field dependent corrections. And the entanglement entropy should also not change in a dramatic way, exhibiting the  $A \log(A)$  behaviour characteristic of a Fermi surface with small correction due to the magnetic field. It is also worth mentioning that for a Fermi liquid in the presence of a small magnetic field the spin of the quasi particles results in the phenomenon of Pauli paramagnetism, see [41]. If  $\epsilon_f$  is the Fermi energy at zero temperature and  $\delta E$  the Zeeman splitting due to the magnetic field then the resulting magnetization is linear in the magnetic field as long

as

$$\delta E/\epsilon_f \ll 1, \quad (4.1)$$

and this effect persists at small non-zero temperature <sup>12</sup>,

$$T/\epsilon_f \ll 1. \quad (4.2)$$

In addition there are de Haas-van Alphen oscillations in the magnetisation and other properties as the magnetic field is varied, see [15].

In contrast the introduction of a small magnetic field in the dilaton system can have a dramatic effect on the IR behaviour as we have already discussed. Here we will study some additional aspects of the resulting thermodynamics.

In our system the role of the Fermi energy is played by the chemical potential  $\mu$ . Let us start with the purely electric theory first at a small temperature  $T$

$$T/\mu \ll 1 \quad (4.3)$$

As discussed in [3], [26] the entropy density  $s = S/V$  goes like

$$s \sim N^2 T^{\frac{2\beta}{2\gamma-1}}. \quad (4.4)$$

Under the scaling symmetry equations, (2.20), (2.21), (2.22),  $s$  has dimensions of  $L^{\theta-2}$ , where  $\theta$  is defined in eq.(2.29) and  $L$  transforms in the same way as the  $(x, y)$  coordinates do in eq.(2.22). Thus  $\theta$  is the exponent related to hyperscaling violation.

Now we can consider introducing a small magnetic field  $Q_m$ . Since the stress energy of the electromagnetic field is quadratic in  $Q_m^2$  this should result in a correction to the entropy which is of order  $Q_m^2$ . The scaling symmetry eq.(2.21), eq.(2.22) then fixes the resulting temperature dependence of this correction so that  $s$  is given by

$$s \sim N^2 \mu^2 \left( \frac{T}{\mu} \right)^{\frac{2\beta}{2\gamma-1}} \left( 1 + s_1 \left( \frac{Q_m}{\mu^2} \right)^2 \left( \frac{T}{\mu} \right)^{\frac{4\alpha k}{2\gamma-1}} \right) \quad (4.5)$$

where  $k$  is defined in eq.(2.11), eq.(2.12) and  $s_1$  is a  $\mu$  independent constant. We see that the magnetic field can be regarded as a small perturbation only for temperatures meeting the condition

$$\left( \frac{Q_m}{\mu^2} \right)^2 \left( \frac{T}{\mu} \right)^{\frac{4\alpha k}{2\gamma-1}} \ll 1 \quad (4.6)$$

We have numerically verified that the coefficient  $s_1$  indeed does not vanish for generic values of  $(\alpha, \delta)$ .

The condition eq.(4.6) is in agreement with the discussion of section §2 where we found that the magnetic field is irrelevant or relevant in the IR depending on the sign of  $\alpha k$ . Since  $2\gamma - 1 > 0$ , eq.(2.18), we see from eq.(4.5) that when  $\alpha k > 0$  the effects of the magnetic field on the entropy vanish as  $T \rightarrow 0$ . On the other hand when  $\alpha k < 0$  these effects grow as  $T \rightarrow 0$ .

---

<sup>12</sup>In particular the temperature does not have to be smaller than  $\delta E$  as long as eq.(4.1), eq.(4.2) are satisfied.



#### 4.1 More on Case II.

One region of the parameter space where  $\alpha k < 0$  corresponds to Case II. As discussed in §2 in this case the resulting geometry for  $T = 0$  in the deep IR is of the extreme RN type and the entropy at extremality does not vanish. From eq.(3.11) this entropy is given by

$$S = s_0 V N^2 \mu^2 \left( \frac{Q_m}{\mu^2} \right)^{\frac{\alpha+\delta}{2\alpha}} \quad (4.7)$$

where  $s_0$  is a dimensionless constant,  $V$  is the volume and we have used eq.(2.30). The remaining region of parameter space where  $\alpha k < 0$  corresponds to Case III. For this case as discussed in §2 our analysis is not complete. If the IR in the gravity theory is an attractor of the magnetic scaling type described in 3.3 then the entropy vanishes at extremality.

It is also worth commenting on the behaviour of some of the other thermodynamic variables for Case II. We start with the case where both  $Q_m, T$  vanish, then first introduce a small  $Q_m/\mu^2 \ll 1$  and finally a small temperature. The temperature we consider meets the condition  $T/\mu \ll 1$ . In fact it is taken small enough to meet the more stringent condition

$$\frac{Q_m^2}{\mu^4} \gg \left( \frac{T}{\mu} \right)^{\frac{-4\alpha k}{2\gamma-1}} \quad (4.8)$$

so that eq.(4.6) does not hold and the near horizon geometry is that of a near-extremal RN black brane at a small non-zero temperature.

The discussion of thermodynamics is conceptually simplest if we think of the gravity solution being asymptotic in the deep UV to AdS space with a possible non-normalisable mode for the dilaton turned on, as was discussed in 2.1. In the absence of a magnetic field the dual field theory is a relativistic theory with the coupling constant dual to the dilaton being turned on and thus scale invariance being broken. The energy density  $\rho$  and pressure  $P$  for such a system at zero temperature are given by

$$\rho = c_1 N^2 \mu^3 + \rho_0 \quad (4.9)$$

$$P = \frac{c_1}{2} N^2 \mu^3 - \rho_0 \quad (4.10)$$

where the  $\rho_0$  term arises due to the cosmological constant induced by to the breaking of scale invariance when the non-normalisable mode of the dilaton is turned on.

On introducing a small magnetic field the geometry changes for Case II significantly in the deep IR. However one expects that the resulting change in  $\rho, p$ , which are determined by the normalisable mode of gravity at the boundary, is small. Since the stress-energy in the bulk changes at quadratic order in  $Q_m$ , as was discussed above, this correction should be of order  $Q_m^2$ . Thus the pressure, working still at

zero temperature, would become

$$P = \frac{c_1}{2} N^2 \mu^3 - \rho_0 + a_1 N^2 \frac{Q_m^2}{\mu} \quad (4.11)$$

where  $a_1$  is a dimensionless constant. The resulting magnetisation can be obtained using the thermodynamic relation

$$SdT + Nd\mu - VdP + MdQ_m = 0. \quad (4.12)$$

Keeping  $T = 0$  and  $\mu$  fixed gives

$$\frac{M}{V} = \frac{dP}{dQ_m} = 2a_1 N^2 \frac{Q_m}{\mu} \quad (4.13)$$

We expect this magnetisation to be diamagnetic.

Introducing a small temperature next will result in a temperature dependence in the pressure and the magnetisation. The change in the pressure keeping  $\mu, Q_m$  fixed and increasing  $T$  slightly is given from eq.(4.12) by

$$\Delta P = \int s dT = s_0 N^2 \mu^2 \left( \frac{Q_m}{\mu^2} \right)^{\frac{\alpha+\delta}{2\alpha}} T \quad (4.14)$$

where we have used eq.(4.7). Adding this to eq.(4.11) gives the total pressure to be

$$P = \frac{c_1}{2} N^2 \mu^3 - \rho_0 + a_1 N^2 \frac{Q_m^2}{\mu} + s_0 N^2 \mu^2 \left( \frac{Q_m}{\mu^2} \right)^{\frac{\alpha+\delta}{2\alpha}} T \quad (4.15)$$

The resulting magnetisation also acquires a linear dependence on temperature

$$\frac{M}{V} = 2a_1 N^2 \frac{Q_m}{\mu} + s_0 N^2 \left( \frac{\alpha+\delta}{2\alpha} \right) T \left( \frac{Q_m}{\mu^2} \right)^{\frac{\delta-\alpha}{2\alpha}} \quad (4.16)$$

Notice that in Case II  $|\alpha| > \delta$  and therefore the exponent  $\frac{\delta-\alpha}{2\alpha}$  in the second term on the RHS is negative. Since  $Q_m/\mu^2 \ll 1$  this means that the coefficient of the term linear in  $T$  in the magnetisation is enhanced. As a result at a small temperature of order

$$\frac{T}{\mu} \sim \left( \frac{Q_m}{\mu^2} \right)^{\frac{3\alpha-\delta}{2\alpha}} \quad (4.17)$$

this term will become comparable to the zero temperature contribution.

A case of particular interest is when  $\alpha = -3\delta$ . This corresponds to  $\theta = 1$ , eq.(2.29), and gives rise to the logarithmic enhancement of entropy eq.(1.1). The pressure and magnetisation etc can be obtained for this case by substituting this relation between  $\alpha, \delta$  in the the equations above.

Let us end this section some comments. It is important to note that after turning on the magnetic field the state is still compressible. The compressibility is defined

by  $\kappa = -\frac{1}{V}\frac{\partial V}{\partial P}|_{TQ_mN}$  and can be related to the change in charge or number density  $n$  as  $\mu$  is changed,

$$\kappa = \frac{1}{n^2}\left(\frac{\partial n}{\partial \mu}\right)|_{TQ_m} \quad (4.18)$$

From eq.(4.12) and eq.(4.15) we see that

$$n = \frac{\partial P}{\partial \mu}|_{TQ_m} = \frac{3}{2}c_1 N^2 \mu^2 + \dots \quad (4.19)$$

where the first term on the RHS arises from the first term in  $P$  in eq.(4.15) and the ellipses denote corrections which are small. Thus the charge density is only slightly corrected by the addition of  $Q_m$  and therefore the state remains compressible. Our discussion above for the magnetisation etc has been for Case II. The analysis in case I where the magnetic field is irrelevant in the IR is straightforward. For Case III we do not have a complete analysis of what happens in the gravity theory in the deep IR. A candidate attractor was identified in §3, if this attractor is indeed the IR end point then starting from it the resulting thermodynamics can be worked out at small  $Q_m, T$  along the lines above.

## 5. Entanglement Entropy

The entanglement entropy for the hyperscaling violating metrics we have been considering has already been worked out in [10], see also [11]. Knowing these results, the behaviour of the entanglement entropy for our system of interest, in the presence of a small magnetic field, can be easily deduced.

To keep the discussion self contained we first review the calculation of the entanglement entropy for hyperscaling violating metrics and then turn to the system of interest.

### 5.1 Entanglement Entropy in Hyperscaling Violating Metrics

We will be considering a metric of the form

$$ds^2 = -r^{2\gamma} dt^2 + \frac{dr^2}{r^{2\gamma}} + r^{2\beta}(dx^2 + dy^2) \quad (5.1)$$

(this is the same form as eq.(2.11) except that we have dropped the constant  $C_a^2$  by appropriately scaling the metric). In the discussion below it will be useful to think of this metric as arising in the IR starting with an AdS metric in the UV. This could happen for an appropriately chosen potential as was discussed in §2, [26]. The field theory of interest then lives on the boundary of AdS space. For simplicity we will restrict ourselves to a circular region  $\mathbf{R}$  in the field theory of radius  $L$ . The boundary of this region in the field theory  $\partial\mathbf{R}$  is a circle of radius  $L$ . To compute the entanglement entropy of  $\mathbf{R}$  we work on a fixed constant time slice and find the surface

in the bulk which has minimum area subject to the condition that it terminates in  $\partial\mathbf{R}$  at the boundary of AdS. The entanglement entropy is then given by [34],[35].

$$S_{EE} = \frac{A_{min}}{4G_N} \quad (5.2)$$

where  $A_{min}$  is the area of this surface.

We will work in a coordinate system of the form eq.(2.4) which as  $r \rightarrow 0$  becomes eq.(5.1) and as  $r \rightarrow \infty$  becomes AdS space

$$ds^2 = r^2(-dt^2) + \frac{dr^2}{r^2} + r^2(dx^2 + dy^2). \quad (5.3)$$

Replacing  $(x, y)$  by  $(\xi, \theta)$  the metric eq.(2.4) can be rewritten as

$$ds^2 = -a^2 dt^2 + \frac{dr^2}{a^2} + b^2(d\xi^2 + \xi^2 d\theta^2). \quad (5.4)$$

We expect the minimum area bulk surface to maintain the circular symmetry of the boundary circle. Such a circularly symmetric surface has area

$$A_{bulk} = 2\pi \int \sqrt{b^2 \left( \frac{d\xi}{dr} \right)^2 + \frac{1}{a^2}} \xi(r) b(r) dr \quad (5.5)$$

where  $\xi(r)$  is the radius of the circle which varies with  $r$ . To obtain  $A_{min}$  we need to minimise  $A_{bulk}$  subject to the condition that as  $r \rightarrow \infty$ ,  $\xi \rightarrow L$ . The resulting equation for  $\xi(r)$  is

$$\frac{d}{dr} \left( \frac{b^3 \xi \frac{d\xi}{dr}}{\sqrt{b^2 \left( \frac{d\xi}{dr} \right)^2 + \frac{1}{a^2}}} \right) - \sqrt{b^2 \left( \frac{d\xi}{dr} \right)^2 + \frac{1}{a^2}} b = 0. \quad (5.6)$$

Let us note that the circle on the boundary of  $\mathbf{R}$  has area<sup>13</sup>

$$A = 2\pi L \quad (5.7)$$

It is easy to see that as  $r \rightarrow \infty$  the  $b^2 \left( \frac{d\xi}{dr} \right)^2$  term in the square root in eq.(5.5) cannot dominate over the  $\frac{1}{a^2}$  term. The contribution to  $A_{bulk}$  from the  $r \rightarrow \infty$  region can then be estimated easily to give

$$\delta_1 A_{bulk} = A r_{max} \quad (5.8)$$

where  $r_{max}$  is the IR cutoff in the bulk which should be identified with a UV cutoff in the boundary. This is the expected universal contribution to entanglement which arises from very short distance modes entangled across the boundary of  $\mathbf{R}$ .

---

<sup>13</sup>As mentioned earlier we will persist in calling this the area although it is of course the perimeter.

Now one would expect that as  $L$  is increased the bulk surface penetrates deeper into the IR eventually entering the scaling region eq.(5.1). For large enough  $L$  one expects that the radial variable  $\xi$  stays approximately constant in the UV and undertakes most of its excursion from  $L$  to 0 in this scaling region. We will make these assumption here and proceed. These assumptions can be verified numerically for the interesting range of parameters and we will comment on this further below.

With these assumptions the contribution from the scaling region for the minimal area surface  $\delta_2 A_{bulk}$  can be estimated by a simple scaling argument. We can neglect the change in  $\xi$  before the surface enters the scaling region and take its value at the boundary of the scaling region<sup>14</sup> which we denote as  $\xi_0$  to be  $L$ . Under the scaling symmetry eq.(2.20)-eq.(2.22), which takes

$$r \rightarrow \lambda r, \xi \rightarrow \lambda^{1-\beta-\gamma} \xi, \quad (5.9)$$

we see from eq.(5.5) that

$$\delta_2 A_{bulk} \rightarrow \lambda^{2(1-\gamma)} \delta_2 A_{bulk} \quad (5.10)$$

Now by choosing  $\lambda$  in eq.(5.9) to be

$$\lambda = L^{\frac{1}{\gamma+\beta-1}} \quad (5.11)$$

we can set the rescaled value for  $\xi_0$  to be unity. In terms of the rescaled variable the minimisation problem has no scale left and  $\delta_2 A_{bulk}$  must be order unity. This tells us that when  $\xi_0 = L$

$$\delta_2 A_{bulk} \sim L L^{\frac{\gamma-\beta-1}{\gamma+\beta-1}}. \quad (5.12)$$

Note also that with  $\xi_0$  set equal to unity the surface would reach a minimum value at a radial value of  $r_{min}$  which is of order unity. Thus before the rescaling

$$r_{min} \sim \lambda = L^{-(\frac{1}{\beta+\gamma-1})}. \quad (5.13)$$

Now we are ready to consider different regions in the  $(\gamma, \beta)$  parameter space. From eq.(2.12) we see that  $\beta > 0$  and from eq.(2.18) that  $\gamma > 1/2$ .

- $\gamma > 1 + \beta$ : In this case we see from eq.(5.12) and (5.8) that  $\delta_2 A_{bulk} > \delta_1 A_{bulk}$  for sufficiently big  $L$  and fixed UV cutoff  $r_0$ . Thus the dominant contribution to the area for sufficiently big  $L$  comes the scaling region. The entanglement is then given by

$$S_{EE} \sim N^2 (L\mu) (L\mu)^{\frac{\gamma-\beta-1}{\gamma+\beta-1}} \quad (5.14)$$

with an additional term proportional to  $L$  in units of the UV cutoff  $r_0$ . In eq.(5.14) we have introduced the scale  $\mu$  to make up the dimensions. We

---

<sup>14</sup>By the boundary of the scaling region we mean the region where the metric begins to significantly depart from eq.(5.1). This happens as we go to larger values of  $r$ ; for even larger values the metric becomes AdS space.

remind the reader that this scale stands for the chemical potential which is the only length scale in the boundary theory. We see from eq.(5.14) that the entanglement grows with  $L$  with a power faster than unity. Also notice that from eq.(5.13)  $r_{min}$  decreases with increasing  $L$  in accord with our expectation that the surface penetrates further into the scaling region as  $L$  is increased.

- A special case of importance is when  $1 + \beta = \gamma$ . Here the term  $(L\mu)^{\frac{\gamma-\beta-1}{\gamma+\beta-1}}$  is replaced by a log, [10], resulting in eq.(5.14) being replaced by

$$S_{EE} \sim N^2(L\mu) \log(L\mu) \quad (5.15)$$

- $1 + \beta > \gamma > 1 - \beta$  : In this case we see from eq.(5.12) and eq.(5.8) that the contribution  $\delta_2 A_{bulk}$  grows with  $L$  with a power less than unity and therefore the contribution made by the scaling region to the total area is less significant than  $\delta_1 A$  which is linear in  $L$ . In this region of parameter space the entanglement entropy is therefore dominated by the short distance contributions and given by

$$S_{EE} \sim N^2 \frac{L}{a} \quad (5.16)$$

where  $a = \frac{1}{r_{max}}$  is an UV cutoff in the system.

- $\gamma < 1 - \beta$ : In this case  $r_{min}$  does not decrease with increasing  $L$ , actually the surface stops entering the scaling region and our considerations based on the scaling symmetry are not relevant. The entanglement entropy is again given by eq.(5.16).

One can calculate the minimal area surface numerically for cases when  $\gamma > 1 + \beta$  and also  $1 + \beta > \gamma > 1 - \beta$ . This gives agreement with the above discussion including the scaling behaviour for  $r_{min}$  eq.(5.13) in these regions of parameter space.

Let us make some more comments now. In the case where the near horizon geometry is of extreme RN type, i.e.,  $AdS_2 \times R^2$  we have  $\beta = 0, \gamma = 1$ . This case needs to be dealt with separately. Here the entanglement entropy scales like the volume and equals the Beckenstein-Hawking entropy of the corresponding region in the boundary theory.

$$S_{EE} \sim N^2(L\mu)^2 \quad (5.17)$$

The discussion in §2 was in terms of the parameters  $(\alpha, \delta)$  while here we have used  $(\beta, \gamma)$ . The relation between these parameters is obtained from eq.(2.13) and summarised in Table 1. We see that  $\gamma > 1 + \beta$  corresponds to Region D. The line  $\gamma = 1 + \beta$  corresponds to  $\alpha = -3\delta$  at the interface between D and E. The condition  $1 + \beta > \gamma > 1 - \beta$  corresponds to A and E and finally  $\gamma < 1 - \beta$  to B and C.

---

<sup>15</sup>We should note that the scaling argument tells us that  $r_{min}$  does decrease with increasing  $L$ , eq.(5.13), so that the surface does get further into the scaling region as  $L$  increases.

## 5.2 Entanglement with a Small Magnetic Field

We are now ready to consider the effects of a small magnetic field. The behaviour of the gravity solutions was discussed in §2 where it was shown that the analysis breaks up into various cases. In all cases we will take the solution to approach AdS space in the UV. The resulting behaviour of the solution was discussed for the various cases in subsection 3.4. For  $r \gg \mu$  the solution is  $AdS$  space while for  $r_* \ll r \ll \mu$  it is of electric scaling type ( $r_*$  is defined in eq.(3.15)). What happens for  $r \ll r_*$  depends on the various cases.

- Case II.  $|\alpha| > \delta$ : In this case the geometry for  $r \ll r_*$  is  $AdS_2 \times R^2$ . Let us start with a boundary circle of very small radius and slowly increase its size. When the radius  $L\mu \ll 1$  the entanglement entropy is given by eq.(5.16). When  $L\mu \sim 1$  the surface begins to penetrate the electric scaling region and as  $L$  increases we see from eq.(5.13) that  $r_{min}$  decreases. When  $r_{min}$  reaches  $r_*$  the surface begins to enter the region where the magnetic field has an appreciable effect on the geometry. Using eq.(5.13) this corresponds to

$$L \sim L_* = \frac{1}{\mu} \left( \frac{Q_e^2}{Q_m^2} \right)^{-\frac{1}{(4\alpha k)(\beta+\gamma-1)}}. \quad (5.18)$$

For

$$L_* \gg L \gg \frac{1}{\mu} \quad (5.19)$$

the entanglement entropy is given by the calculation in the electric solution. Thus for  $-3\delta < \alpha < -\delta$  it grows faster than  $L$  with an additional fractional power while for  $\alpha = -3\delta$  it is logarithmically enhanced. For other values of  $(\alpha, \delta)$  which lie in this region the entanglement entropy is proportional to  $L$  and is dominated by the UV contribution.

Finally, when  $L \gg L_*$  the surface enters into the near-horizon  $AdS_2 \times R^2$  geometry. Now the entanglement entropy grows like  $L^2$  and is given by

$$S \sim L^2 N^2 \mu^2 \left( \frac{Q_m}{\mu^2} \right)^{\frac{\alpha+\delta}{2\alpha}} \quad (5.20)$$

This is an expression analogous to the Beckenstein-Hawking entropy, eq.(4.7), but with  $L^2$  now being the volume of the region of interest. For the case of special interest,  $\alpha = -3\delta$ , this becomes

$$S \sim L^2 N^2 \mu^2 \left( \frac{Q_m}{\mu^2} \right)^{\frac{1}{3}}. \quad (5.21)$$

- Case III.  $0 < \alpha < \delta$ : In this case the magnetic field is important at small  $r$ . For  $L_* \gg L \gg \frac{1}{\mu}$  the entanglement is given by the electric theory, it goes

like eq.(5.16) and arises dominantly due to short distance correlations. The geometry in the deep IR could be the magnetic scaling solution discussed in subsection 3.3. If this is correct for  $L \gg L_*$  the entanglement will continue to go like eq.(5.16).

- Case I.  $-\delta < \alpha < 0$ : In this case the magnetic field is not important in the IR and the the entanglement entropy is given by eq.(5.16) both when  $L < \frac{1}{\mu}$  and  $L > \frac{1}{\mu}$ .

## 6. Concluding Comments

In this paper we have studied a system of gravity coupled to an Abelian gauge field and a dilaton. This system is of interest from the point of view of studying fermionic matter at non-zero charge density. Some of our key results were summarised in §1. We end in this section with some concluding comments.

- For the case  $|\alpha| > \delta$  (Case II in our terminology) we saw that the magnetic field is a relevant perturbation in the IR and the inclusion of a small magnetic field changes the behaviour significantly making the zero temperature thermodynamic entropy extensive and the entanglement grow like the volume. In particular this happens along the line  $\alpha = -3\delta$  ( $\theta = 1$ , eq.(2.29)), where the electric theory has an entanglement entropy of the form eq.(1.1) suggesting the presence of a Fermi surface. Our results suggest that the addition of even a small magnetic field renders the putative Fermi surface unstable. More generally our result shows that the state of matter described by the electric scaling solution for this case anti-screens the effects of the magnetic field.
- It is well known that an extensive ground state entropy can arise in the presence of a magnetic field due to partially filled Landau levels. If this happens the entropy scales like  $Q_m$  while, in contrast, for the dilaton system the dependence on the the magnetic field is typically more exotic, eq.(5.20). E.g., with  $\alpha = -3\delta$  the entropy goes like  $Q_m^{1/3}$ , eq(5.21). Such a non-trivial exponent suggests that the ground state is more interesting and exotic.
- A notable feature about how the entanglement entropy behaves in all the cases we have studied is that it never decreases in the IR, i.e., as one goes to regions of larger and larger size ( $L$ ) in the boundary. For instance, consider the case where  $-3\delta \leq \alpha < -\delta$ . In this case for very small  $L$  is it given by eq.(5.16) and dominated by short distance correlations of the CFT. At intermediate values of  $L$ , meeting the condition eq.(5.19), it goes like eq.(5.14) and is enhanced compared to the  $L$  dependence by an additional fractional power of  $L$  or a  $\log(L)$ , eq.(5.15). Finally at very large values of  $L$  it grows like the volume  $L^2$ ,



eq.(5.17). We see that as  $L$  increases the entanglement increases monotonically<sup>16</sup>. In other cases while the detailed behaviour is different this feature is still true. These observations are in agreement with [42] where a renormalised version of the entanglement entropy was defined and it was suggested that in  $2 + 1$  dimensions this entropy would monotonically increase. It is easy to see that the behaviour of the entanglement entropy we have found implies that the renormalised entanglement entropy of [42] is monotonic and increasing.

- In [26] the behavior of a probe fermion in the bulk in the electric hyperscaling violating geometry was discussed. This corresponds to calculating the two point function of a gauge invariant fermionic correlator in the boundary. It is notable that the region in parameter space where Fermi liquid behaviour was found to occur for this correlator is exactly the region  $|\alpha| > \delta$  for which we have found that the geometry flows to an  $AdS_2 \times R^2$  endpoint in the IR<sup>17</sup>. It would be worth understanding this seeming coincidence more deeply. It is also worth mentioning that in [26] marginal Fermi liquid behaviour was found when  $|\alpha| = \delta$ . This region lies at the boundary of the region  $|\alpha| > \delta$  where an  $AdS_2 \times R^2$  endpoint arise<sup>18</sup>.
- Our focus in this paper was on taking an electrically charged system and including a small magnetic field. However, it is worth pointing out that the magnetic solutions with no electric field present ( $Q_e = 0$ ) are also of considerable interest in their own right. These solutions can be obtained by taking

$$Q_e \rightarrow Q_m \tag{6.1}$$

and  $\alpha \rightarrow -\alpha$  in the solutions eq.(2.12), eq.(2.13). For a choice of parameters, which now meet the condition  $\alpha = 3\delta$ , the resulting entanglement entropy has the form eq.(1.1) which suggests the presence of a Fermi surface even though the charge density is now vanishing. It would be worth understanding the resulting state better in the field theory. The transformation eq.(6.1) is an electromagnetic duality transformation, and should act by exchanging charged particles with vortices in the field theory[43],[44]. These vortices perhaps form a Fermi surface resulting in the logarithmic enhancement of the entropy.

---

<sup>16</sup>Our scaling argument does not directly fix the sign of the entanglement entropy in eq.(5.14) and eq.(5.15). However it is clear that the sign must be positive since the corresponding contribution to the surface area is bigger than the contribution from the UV for fixed  $r_{max}$  as  $L \rightarrow \infty$ , and the total surface area must be positive.

<sup>17</sup>The remaining region  $|\alpha| < \delta$  does not exhibit Fermi liquid behaviour, this includes Case I of §2 where the magnetic field is irrelevant and also Case III of §2 where it is relevant but where we have not identified a definite IR end point to which the solution flows.

<sup>18</sup>In fact the nature of the attractor changes at this boundary. E.g. in the purely electric case when  $\alpha = -\delta$  the dilaton is a flat direction of the attractor potential and not fixed to a unique value in the IR, similarly for  $\alpha = \delta$  in the purely magnetic case.

- We have not included an axion field in our analysis. Such a field is natural to include once the dilaton is present and it can have important consequences once the magnetic field is also turned on as was discussed in [23]. For example it was shown in [23] for the case  $\delta = 0$  that in the presence of the axion the entropy at extremality continues to vanish in the presence of a magnetic field. Once the axion is included we need to allow for the potential to also depend on it, this leads to considerable choice in the kinds of models one can construct. To remove some of this arbitrariness it would be worth including the axion within the context of models which arise in string theory or at least gauged supergravity.
- More generally, the time seems now ripe to systematically embed models of this type in string theory and supergravity. Some papers in this direction have already appeared [45], [46],[47],[48], [49],[50]. It would be worth understanding these constructions better and also gaining a better understanding of their dual field theory descriptions.

### Acknowledgements

We are grateful to K. Damle, S. Kachru, G. Mandal, S. Minwalla, T. Takayanagi and V. Tripathy for discussion. SPT thanks the organisers of the Strings Discussion meeting at the ICTS, Bangalore, for a stimulating conference and acknowledges the support of a J.C. Bose Fellowship from the Dept. of Science and Technology, Govt. of India. We all acknowledge the support of DAE, Government of India and most of all are grateful to the people of India for generously supporting research in string theory.

## A. Appendix : Numerical Interpolation.

In this appendix we consider Case II solutions which were discussed in section 3.2 and establish that the deep IR solution is indeed  $AdS_2 \times R^2$ . We establish this numerically by integrating outwards from the  $AdS_2 \times R^2$  near horizon solution discussed in subsection 3.2 and showing that the system approaches the electric scaling solution. For a suitable potential we find that the electric scaling solution in turn finally asymptotes to  $AdS_4$  in the UV. Our numerical work is done using the Mathematica package.

We divide the discussion into three parts. In the first part we identify two perturbations in the  $AdS_2 \times R^2$  region that grow towards the UV. In the second part, by choosing an appropriate combination of these two perturbations, we numerically integrate outwards taking the scalar potential to be  $V(\phi) = -|V_0|e^{2\delta\phi}$ , eq.(2.3). At moderately large radial distances we get the electric scaling solution. In the last part, taking the potential to be of the form  $V(\phi) = -2|V_0| \cosh(2\delta\phi)$ <sup>19</sup>, we continue the numerical integration towards larger  $r$  and show that the geometry asymptotes to  $AdS_4$ .

### A.1 The perturbations

To identify the perturbations in the  $AdS_2 \times R^2$  solution discussed in 3.2 we consider perturbations of this solution of the following form for the metric components and the dilaton,

$$a(r) = C_a r [1 + a_{c1} r^\nu + \mathcal{O}(r^{2\nu})] \quad (\text{A.1})$$

$$b(r) = b_0 [1 + b_{c1} r^\nu + \mathcal{O}(r^{2\nu})] \quad (\text{A.2})$$

$$\phi(r) = \phi_0 + \log [1 + \phi_{c1} r^\nu + \mathcal{O}(r^{2\nu})] . \quad (\text{A.3})$$

Note that this is a perturbation series in  $r^\nu$  which is valid in the near horizon region where  $r \ll 1$ . Equations (2.7-2.10) can be solved to leading order in  $r^\nu$  to find perturbations which are relevant towards the UV, i.e with  $\nu > 0$ . We find two such perturbations parametrized by their strengths  $\phi_{c1}^{(1)}, a_{c1}^{(2)}$  which are given below :

$$a_{c1}^{(1)} = \frac{2\delta}{1 + \alpha^2 - \delta^2 + \sqrt{1 + 4\alpha^2 - 4\delta^2}} \phi_{c1}^{(1)} \quad (\text{A.4})$$

$$b_{c1}^{(1)} = 0 \quad (\text{A.5})$$

$$\nu_1 = \frac{1}{2}(-1 + \sqrt{1 + 4\alpha^2 - 4\delta^2}) \quad (\text{A.6})$$

---

<sup>19</sup>Note, for this last part we present results for the case where  $\alpha > \delta$  so that in the electric scaling solution  $\phi \rightarrow \infty$  in the deep IR. As a result the modified potential  $-2|V_0| \cosh(2\delta\phi)$  can be approximated by  $-|V_0|e^{2\delta\phi}$  in the IR. In the UV we then find that the modified potential allows for an  $AdS_4$  solution. A similar analysis can be done when  $\alpha < -\delta$ , using a suitably modified potential.

and

$$b_{c1}^{(2)} = -\frac{3(-2 + \alpha^2 - \delta^2)}{2(-2 + \alpha^2 - 2\delta^2)} a_{c1}^{(2)} \quad (\text{A.7})$$

$$\phi_{c1}^{(2)} = -\frac{3\delta}{(-2 + \alpha^2 - 2\delta^2)} a_{c1}^{(2)} \quad (\text{A.8})$$

$$\nu_2 = 1 \quad (\text{A.9})$$

Note that  $b_{c1}^{(1)}$  vanishes in the first of the above perturbations, as a result the first correction to  $b(r)$  starts at second order. Actually, we found it important to go to second order in the first of the above perturbations for carrying out the numerical integration satisfactorily. We will not provide the detailed expressions for these second order corrections here since they are cumbersome.

## A.2 Scaling symmetries

The system of equations eq.(2.7)-eq.(2.10) has two scaling symmetries.

$$a^2 \rightarrow \lambda_1 a^2, \quad r^2 \rightarrow \lambda_1 r^2 \quad (\text{A.10})$$

$$(Q_e^2, Q_m^2) \rightarrow \lambda_2 (Q_e^2, Q_m^2), \quad b^2 \rightarrow \lambda_2 b^2 \quad (\text{A.11})$$

The first scaling symmetries can be used to set <sup>20</sup>  $a_{c1}^{(2)} = -1$ . The second scaling symmetry can then be used to set  $Q_e = 1$ . In addition we can choose units so that  $|V_0| = 1$ . With these choices the system of equations has two parameters,  $\phi_{c1}^{(1)}$ , which characterises the first perturbation, eqn. (A.4), and  $Q_m$ . Numerical analysis shows that for a given choice of  $Q_m \ll \mu^2$ ,  $\phi_{c1}^{(1)}$  needs to be tuned very precisely to ensure that the solution flows to the electric scaling solution. Otherwise, for example with the modified potential considered in subsection A.4 below, the solution can flow from the  $AdS_2 \times R^2$  region in the IR directly to  $AdS_4$ , as  $r \rightarrow \infty$ , without passing close to the electric scaling solution at intermediate values of  $r$ .

## A.3 Numerics : $AdS_2 \times R^2$ to the Electric Scaling Solution

We will illustrate the fact that the solution evolves from the  $AdS_2 \times R^2$  geometry to the electric scaling solution once the values of  $\phi_{c1}^{(1)}$  is suitably chosen with one example here. Similar behaviour is found for other values of  $(\alpha, \delta)$ , which lie in Case II <sup>21</sup>

The example we present here has  $\alpha = 1, \delta = 0.6$  (satisfying  $|\alpha| > \delta$ ). We will present the data here for the case when  $Q_m = 10^{-4}$  the behaviour for other values of  $Q_m \ll \mu^2$  is similar. It turns out that in this case we have to fine tune the value of

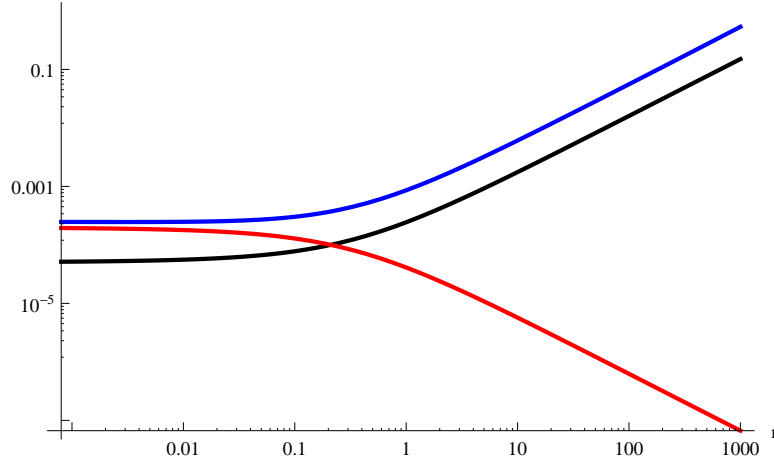
---

<sup>20</sup>We cannot change the sign of  $a_{c1}^{(2)}$  by using the symmetries. The above sign is necessary for the solution to flow to the electric scaling solution in the UV.

<sup>21</sup>The example we choose here has  $\alpha, \delta > 0$ . Similar results are also obtained when  $\alpha < 0, \delta > 0$ .

this parameter to be near  $\phi_{cl}^{(1)} = -0.3173$  so as to obtain an electric scaling solution at intermediate  $r$ .

Evidence for the electric scaling solution can be obtained by examining the relative contributions that various terms make in the effective potential eq.(2.6). In the electric scaling region the contribution that the  $Q_m^2$  dependent term makes must be smaller than the  $Q_e^2$  dependent term and the scalar potential which in turn must scale in the same way. Fig.(3) shows the different contributions to  $V_{eff}$  made by the terms,  $e^{-2\alpha\phi}Q_e^2$ ,  $e^{2\alpha\phi}Q_m^2$  and  $b^4(r)\frac{e^{2\delta\phi}}{2}$  in a Log-Log plot. Clearly the  $Q_e^2$  term is growing as the same power of  $r$  as the scalar potential  $e^{2\delta\phi}$  term and  $Q_m^2$  is subdominant.



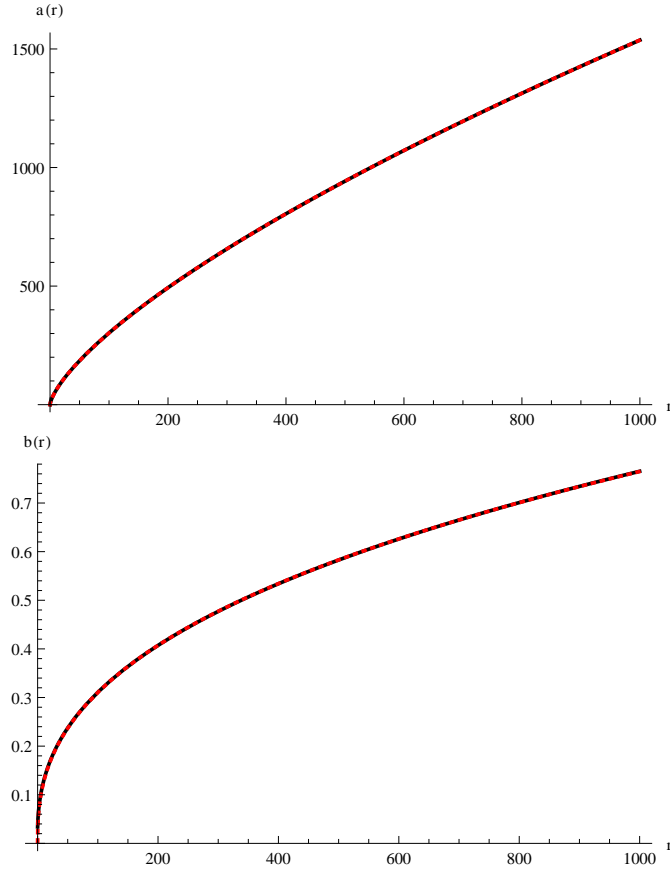
**Figure 3:** Different contributions to  $V_{eff}$  in Log-Log plot. Blue→ Scalar Potential  $b^4(r)\frac{e^{2\delta\phi}}{2}$ , Black→  $Q_e^2 e^{-2\alpha\phi}$  term, Red→  $Q_m^2 e^{2\alpha\phi}$  term.

Fig.(4) and Fig.(5) show the plots of metric components  $a(r)$ ,  $b(r)$  and the scalar  $\phi(r)$  obtained numerically. Each of them is fitted to a form given in eq(2.12). We see that the fitted parameters agree well with the analytic values for  $\beta$ ,  $\gamma$  and  $k$  obtained from eq.(2.13) with  $(\alpha, \delta) = (1, 0.6)$ . This confirms that the system flows to the electric scaling solution.

#### A.4 Numerics : $AdS_2 \times R^2 \rightarrow$ Electric Scaling $\rightarrow AdS_4$ .

Here we show that on suitably modifying the potential so that the IR behaviour is essentially left unchanged the solution which evolves from the  $AdS_2 \times R^2$  geometry in the deep IR to the electric scaling solution can be further extended to become asymptotic  $AdS_4$  in the far UV.

We will illustrate this for the choice made in the previous subsection:  $(\alpha, \delta) = (1, 0.6)$ ,  $(Q_e = 1, Q_m = 10^{-4})$ . For this choice of  $(\alpha, \delta)$  it is easy to see from eq.(2.12), eq.(2.13) that  $\phi \rightarrow \infty$  in the IR of the electric scaling solution, and from eq.(3.10) that it continues to be big in the  $AdS_2 \times R^2$  geometry once the effects of the magnetic



**Figure 4:** In the top plot,  $a(r) \sim r^\gamma$  with  $\gamma_{Fit} = 0.706$  whereas  $\gamma_{Analytical} = 0.707$ . In the bottom plot,  $b(r) \sim r^\beta$  with  $\beta_{Fit} = 0.391$  whereas  $\beta_{Analytical} = 0.390$ .

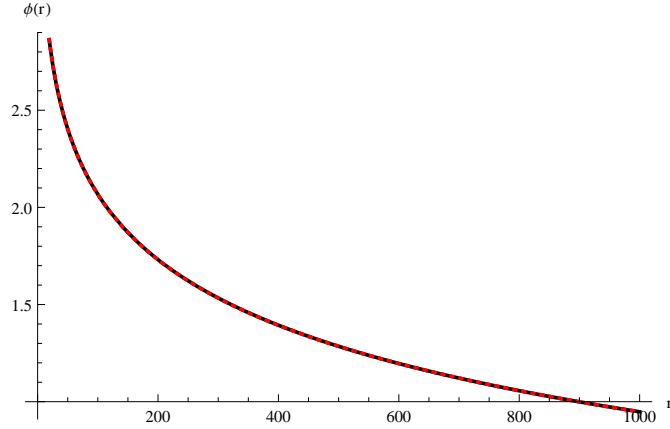


**Figure 5:**  $\phi = k \log[r]$ .  $k_{Fit} = -0.4858$  as compared to  $k_{Analytical} = -0.4878$ .

field are incorporated. We will modify the potential to be

$$V(\phi) = -2|V_0| \cosh(2\delta\phi) \quad (\text{A.12})$$

instead of eq.(2.3). For  $\phi \rightarrow \infty$  we see that this makes a small change, thus our analysis in the previous subsection showing that the solution evolves from the  $AdS_2 \times R^2$  geometry to the electric scaling solution will be essentially unchanged. However, going to larger values of  $r$  the modification in the potential will become important. This modified potential has a maximum for the dilaton at  $\phi = 0$  and a corresponding  $AdS_4$  solution with <sup>22</sup>  $R_{AdS}^2 = -\frac{3}{V_0}$ . We find by numerically integrating from the IR that the solution evolves to this  $AdS_4$  geometry in the UV.

To see this first consider a plot of the three different contributions to  $V_{eff}$  proportional to  $e^{-2\alpha\phi}Q_e^2$ ,  $e^{2\alpha\phi}Q_m^2$  and  $b^4(r) \cosh(2\delta\phi)$  shown in Fig(6). We see that there are three distinct regions. In the far IR  $AdS_2 \times R^2$  region, the three contributions are comparable. At intermediate  $r$  where we expect an electric scaling solution on the basis of the discussion of the previous subsection the magnetic field makes a subdominant contribution and the other two contributions indeed scale in the same way. Finally at very large  $r$ , in the far UV, the cosmological constant is dominant as expected for an  $AdS_4$  solution.

We also show the metric components  $a(r), b(r)$  in a Log-Log plot in Fig(7) and (8). Once again, we can see three distinct slopes for  $a, b$ , corresponding to three different regions in the solution. In the  $AdS_4$  region, as  $r \rightarrow \infty$ , numerically fitting the behaviour gives  $a(r), b(r) \sim r^{0.99}$  which is in good agreement<sup>23</sup> with the expected linear behaviour. Finally, Fig(8) shows the scalar function  $\phi(r)$  settling to zero with the expected fall-off as  $r \rightarrow \infty$ . These results confirm that the system evolves to  $AdS_4$  in the far UV.

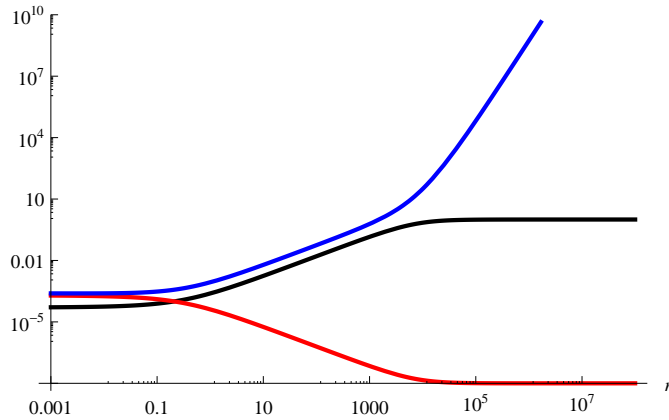


**Figure 6:** Different contributions to  $V_{eff}$  in Log-Log plot. Blue→ Scalar Potential  $b^4(r) \cosh(2\delta\phi)$ , Black→  $Q_e^2 e^{-2\alpha\phi}$  term, Red→  $Q_m^2 e^{2\alpha\phi}$  term.

<sup>22</sup>This example was analysed in [26]. The dilaton lies above the BF bound of the resulting  $AdS_4$  theory for our choice of parameters.

<sup>23</sup>The fit was done for  $r \sim 10^7$ .

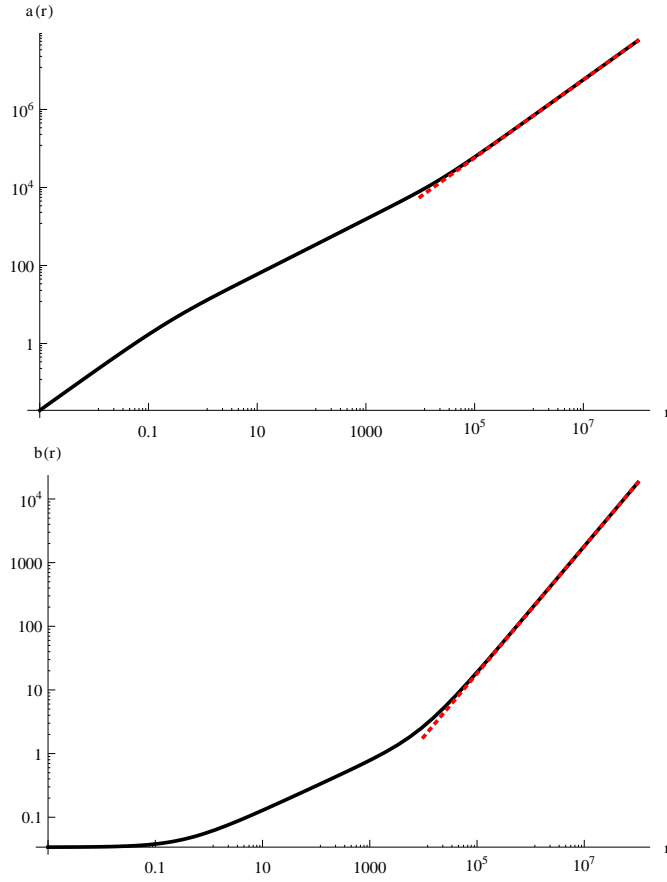


**Figure 7:** In the Log-Log plot both curves show three different slopes for the metric components, which correspond to the three regions  $AdS_2 \times R^2$ , Electric Scaling Region and  $AdS_4$  respectively.

## References

- [1] S. S. Gubser and F. D. Rocha, “Peculiar properties of a charged dilatonic black hole in  $AdS_5$ ,” Phys. Rev. D **81**, 046001 (2010) [arXiv:0911.2898 [hep-th]].
- [2] K. Goldstein, S. Kachru, S. Prakash and S. P. Trivedi, “Holography of Charged Dilaton Black Holes” [arXiv:0911.3586]
- [3] C. Charmousis, B. Gouteraux, B. S. Kim, E. Kiritsis and R. Meyer, “Effective Holographic Theories for low-temperature condensed matter systems,” arXiv:1005.4690 [hep-th].
- [4] L. Huijse and S. Sachdev, “Fermi surfaces and gauge-gravity duality,” Phys. Rev. D **84**, 026001 (2011) [arXiv:1104.5022 [hep-th]].
- [5] M. M. Wolf, “Violation of the entropic area law for Fermions,” Phys. Rev. Lett. **96**, 010404 (2006) [quant-ph/0503219].



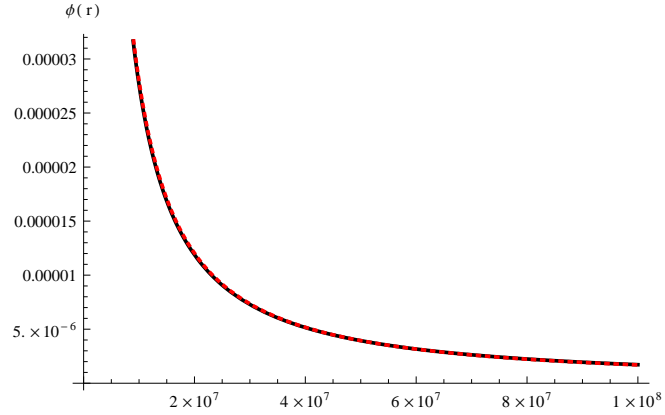


**Figure 8:**  $\phi(r)$  approaches zero like  $r^{-1.22}$  as  $r \rightarrow \infty$ . This agrees with the fall off of non-normalizable component of dilaton in  $AdS_4$ .

- [6] D. Gioev, I. Klich, “Entanglement entropy of fermions in any dimension and the Widom conjecture,” *Phys. Rev. Lett.* **96**, 100503 (2006), arXiv:quant-ph/0504151v4.
- [7] B. Swingle, “Entanglement Entropy and the Fermi Surface”, arXiv:0908.1724v3 [cond-mat.str-el]
- [8] B. Swingle, “Conformal Field Theory on the Fermi Surface”, arXiv:1002.4635v1 [cond-mat.str-el]
- [9] Y. Zhang, T. Grover, A. Vishwanath, “Entanglement entropy of critical spin liquids”, *Phys. Rev. Lett.* **107**, 067202 (2011), arXiv:1102.0350v2 [cond-mat.str-el]
- [10] N. Ogawa, T. Takayanagi and T. Ugajin, “Holographic Fermi Surfaces and Entanglement Entropy,” *JHEP* **1201**, 125 (2012) [arXiv:1111.1023 [hep-th]].
- [11] L. Huijse, S. Sachdev and B. Swingle, “Hidden Fermi surfaces in compressible states of gauge-gravity duality,” *Phys. Rev. B* **85**, 035121 (2012) [arXiv:1112.0573 [cond-mat.str-el]].
- [12] F. Denef, S. A. Hartnoll and S. Sachdev, “Quantum oscillations and black hole ringing,” *Phys. Rev. D* **80**, 126016 (2009) [arXiv:0908.1788 [hep-th]].
- [13] T. Faulkner and N. Iqbal, “Friedel oscillations and horizon charge in 1D holographic liquids,” arXiv:1207.4208 [hep-th].
- [14] S. A. Hartnoll and E. Shaghoulian, “Spectral weight in holographic scaling geometries,” *JHEP* **1207**, 078 (2012) [arXiv:1203.4236 [hep-th]].
- [15] Neil W. Ashcroft, N. David Mermin “Solid State Physics”, Thomson Brooks/Cole, QC176.A83.
- [16] S. -S. Lee, “A Non-Fermi Liquid from a Charged Black Hole: A Critical Fermi Ball,” *Phys. Rev. D* **79**, 086006 (2009) [arXiv:0809.3402 [hep-th]].

- [17] H. Liu, J. McGreevy and D. Vegh, “Non-Fermi liquids from holography,” *Phys. Rev. D* **83**, 065029 (2011) [arXiv:0903.2477 [hep-th]].
- [18] M. Cubrovic, J. Zaanen and K. Schalm, “String Theory, Quantum Phase Transitions and the Emergent Fermi-Liquid,” *Science* **325**, 439 (2009) [arXiv:0904.1993 [hep-th]].
- [19] T. Faulkner, H. Liu, J. McGreevy and D. Vegh, “Emergent quantum criticality, Fermi surfaces, and AdS(2),” *Phys. Rev. D* **83**, 125002 (2011) [arXiv:0907.2694 [hep-th]].
- [20] S. A. Hartnoll, J. Polchinski, E. Silverstein and D. Tong, “Towards strange metallic holography,” *JHEP* **1004**, 120 (2010) [arXiv:0912.1061 [hep-th]].
- [21] T. Faulkner and J. Polchinski, “Semi-Holographic Fermi Liquids,” *JHEP* **1106**, 012 (2011) [arXiv:1001.5049 [hep-th]].
- [22] E. Perlmutter, “Domain Wall Holography for Finite Temperature Scaling Solutions,” arXiv:1006.2124 [hep-th].
- [23] K. Goldstein, N. Iizuka, S. Kachru, S. Prakash, S. P. Trivedi and A. Westphal, “Holography of Dyonically Dilaton Black Branes,” *JHEP* **1010**, 027 (2010) [arXiv:1007.2490 [hep-th]].
- [24] R. Meyer, B. Gouteraux and B. S. Kim, “Strange Metallic Behaviour and the Thermodynamics of Charged Dilatonic Black Holes,” *Fortsch. Phys.* **59**, 741 (2011) [arXiv:1102.4433 [hep-th]].
- [25] B. Gouteraux, B. S. Kim and R. Meyer, “Charged Dilatonic Black Holes and their Transport Properties,” *Fortsch. Phys.* **59**, 723 (2011) [arXiv:1102.4440 [hep-th]].
- [26] N. Iizuka, N. Kundu, P. Narayan and S. P. Trivedi, “Holographic Fermi and Non-Fermi Liquids with Transitions in Dilaton Gravity,” *JHEP* **1201**, 094 (2012) [arXiv:1105.1162 [hep-th]].
- [27] B. Gouteraux and E. Kiritsis, “Generalized Holographic Quantum Criticality at Finite Density,” *JHEP* **1112**, 036 (2011) [arXiv:1107.2116 [hep-th]].
- [28] B. Gouteraux, J. Smolic, M. Smolic, K. Skenderis and M. Taylor, “Holography for Einstein-Maxwell-dilaton theories from generalized dimensional reduction,” *JHEP* **1201**, 089 (2012) [arXiv:1110.2320 [hep-th]].
- [29] L. Bombelli, R. K. Koul, J. Lee and R. D. Sorkin, “A Quantum Source of Entropy for Black Holes,” *Phys. Rev. D* **34**, 373 (1986).
- [30] M. Srednicki, “Entropy and area,” *Phys. Rev. Lett.* **71**, 666 (1993) [hep-th/9303048].
- [31] C. Holzhey, F. Larsen and F. Wilczek, “Geometric and renormalized entropy in conformal field theory,” *Nucl. Phys. B* **424**, 443 (1994) [hep-th/9403108].

- [32] P. Calabrese and J. L. Cardy, “Entanglement entropy and quantum field theory,” J. Stat. Mech. **0406**, P06002 (2004) [hep-th/0405152].
- [33] P. Calabrese and J. L. Cardy, “Entanglement entropy and quantum field theory: A Non-technical introduction,” Int. J. Quant. Inf. **4**, 429 (2006) [quant-ph/0505193].
- [34] S. Ryu and T. Takayanagi, “Holographic derivation of entanglement entropy from AdS/CFT,” Phys. Rev. Lett. **96**, 181602 (2006) [hep-th/0603001].
- [35] S. Ryu and T. Takayanagi, “Aspects of Holographic Entanglement Entropy,” JHEP **0608**, 045 (2006) [hep-th/0605073].
- [36] S. Harrison, S. Kachru and H. Wang, “Resolving Lifshitz Horizons,” arXiv:1202.6635 [hep-th].
- [37] Jyotirmoy Bhattacharya, Sera Cremonini and Annamaria Sinkovics, “On the IR completion of geometries with hyperscaling violation,” [arXiv:1208.1752v1 [hep-th]]
- [38] K. Goldstein, N. Iizuka, R. P. Jena and S. P. Trivedi, Phys. Rev. D **72**, 124021 (2005) [hep-th/0507096].
- [39] E. Shaghoulian, “Holographic Entanglement Entropy and Fermi Surfaces,” JHEP **1205**, 065 (2012) [arXiv:1112.2702 [hep-th]].
- [40] G. T. Horowitz and B. Way, “Lifshitz Singularities,” Phys. Rev. D **85**, 046008 (2012) [arXiv:1111.1243 [hep-th]].
- [41] Philippe Nozieres “Theory of Interacting Fermi Systems”, Addison Wesley Longman Inc., ISBN 0-201-32824-0.
- [42] H. Liu and M. Mezei, arXiv:1202.2070 [hep-th].
- [43] E. Witten, “SL(2,Z) action on three-dimensional conformal field theories with Abelian symmetry,” In \*Shifman, M. (ed.) et al.: From fields to strings, vol. 2\* 1173-1200 [hep-th/0307041].
- [44] S. A. Hartnoll, P. K. Kovtun, M. Muller and S. Sachdev, “Theory of the Nernst effect near quantum phase transitions in condensed matter, and in dyonic black holes,” Phys. Rev. B **76**, 144502 (2007) [arXiv:0706.3215 [cond-mat.str-el]].
- [45] X. Dong, S. Harrison, S. Kachru, G. Torroba and H. Wang, “Aspects of holography for theories with hyperscaling violation,” JHEP **1206**, 041 (2012) [arXiv:1201.1905 [hep-th]].
- [46] K. Narayan, “On Lifshitz scaling and hyperscaling violation in string theory,” Phys. Rev. D **85**, 106006 (2012) [arXiv:1202.5935 [hep-th]].
- [47] H. Singh, JHEP **1207**, 082 (2012) [arXiv:1202.6533 [hep-th]].

- [48] P. Dey and S. Roy, “Lifshitz-like space-time from intersecting branes in string/M theory,” arXiv:1203.5381 [hep-th].
- [49] P. Dey and S. Roy, “Intersecting D-branes and Lifshitz-like space-time,” arXiv:1204.4858 [hep-th].
- [50] E. Perlmutter, “Hyperscaling violation from supergravity,” JHEP **1206**, 165 (2012) [arXiv:1205.0242 [hep-th]].